RESEARCH ARTICLE

The Biosorption of Lead from Aqueous Solutions by a Wood-immobilized Fungal Biosorbent

Zomesh A. Nath Maini[1,*], **Niña Therese B. Flores**[1], **Enrico P. Muñoz**[1]

[1] School of Biology, Ateneo de Manila University, Katipunan Avenue, Loyola Heights, Quezon City 1108, Philippines

Abstract: Lead [Pb(II)] biosorption capacities of immobilized *Talaromyces macrosporus* on *Moringa oleifera* L. wood were compared against pure fungal and pure *M. oleifera* biomass. A Pb(II) contact test of 1000 ug/mL show similar Pb(II) removal of non-immobilized fungal biomass (F) and powdered wood colonized with fungi (WP+F), with WP+F producing more biomass. Powdered sorbents had higher Pb(II) uptake compared to whole sorbents analyzed through ICP-AES, possibly due to increased surface area for Pb(II) binding. FTIR analysis of the F, WP, and WP+F identified hydroxyl, amino, carbonyl, and sulfhydryl functional groups which constitute probable Pb(II)-affinitive binding sites. The biosorbents tested in a Continuous Flow Column (CF) adsorbed Pb(II) at 1000, 2000, and 4000 ug/mL in 30 minutes with the Pb(II) uptake of WP+F producing removal efficiencies at 91-95% regardless of initial Pb(II) concentration. WP+F also showed significantly higher q values than powdered wood (WP) at 42.67 to 184.83 mg/g for the Pb(II) test concentrations. Recovery of Pb(II) from WP+F yielded 99.61% of adsorbed ions from 1000 ug/mL Pb(II), proving Pb(II) entrapment in the sorbent. This is the first study to describe biosorption capacities for *T. macrosporus* and *M. oleifera* softwood along with the wood's viability as an immobilization scaffold. These results show the potential of using *T. macrosporus* immobilized on *M. oleifera* wood as a tool for removal of Pb(II) in wastewater with high Pb(II) concentrations.

Keywords: Fungi, heavy metals, immobilization, biosorption, FTIR

1 Introduction

Lead [Pb(II)] is one of the most potent and toxic heavy metal (HM) pollutants that adversely affects all biological systems (Assi et al., 2016). Its displacement into various habitats due to increased anthropogenic activities in various sectors has made Pb(II) contamination a global ecological and health problem (Wong et al., 2017). Despite efforts and policies that regulate Pb(II) in effluents, many water systems all over the world remain highly polluted with Pb(II) from various sources of contamination (Hauptman et al., 2017; Mirzabeygi et al., 2017). It has therefore become imperative to look for substantial ways of remediating Pb(II) to prevent continued toxic exposure and food chain bioaccumulation (Velkova et al., 2018).

While several conventional means of Pb(II) removal exist, these remain inefficient due to their high costs, low efficiency, and generation of toxic sludge (Ahluwalia and Goyal, 2007; Kapoor and Viraraghavan, 1995). These problems have opened a niche for the use of biological agents such as fungi for the rehabilitation of Pb(II) and various HMs (Dhankhar and Hooda, 2011) which are safer, efficient, and more cost-effective (Velkova et al., 2018). One of these remediation methods is biosorption, the removal or binding of substances from aqueous substrates or solutions using various biological materials (Michalak et al., 2013).

Fungal biosorption is as a method for heavy metal (HM) removal from aqueous substrates which takes advantage of abundant affinitive functional groups of the fungal biomass for the passive sequestration of HMs (Jha et al., 2014; Dhankhar and Hooda, 2011). Several studies have explored the use of fungal biosorbents and their efficacy in the removal of various HMs in aqueous solutions (Ayangbenro and Babalola, 2017). Despite the success in the preparation and testing of fungal biosorbents, their industrial application is limited by several restrictions which include weak mechanical strength, low elasticity, cell mass separation within solid and liquid phase systems, and the difficulty of producing adequate amounts of fungal biomass at reasonable costs (Cai et al., 2016; Das and Adholeya, 2015).

These boundaries can be overcome by immobilization, a process that crosslinks the biomass of choice to a substrate which can change certain chemical characteristics to optimize biosorption capacity (Velkova et al., 2018; Zahmatkesh et al., 2018; Das and Adholeya, 2015). Immobilization has been reported by various HM biosorption studies showing increased HM removal efficiency in solutions treated with immobilized system biosorbents compared to sole microorganisms

or substrates ([Ding et al., 2019](); [Svobodova and Novotny, 2018]()). In this study, *Moringa oleifera* (Lam.) wood was utilized as a scaffold for the immobilization of *Talaromyces macrosporus*, a fungus that has been reported to have extensive Pb(II) removal capacities ([Maini et al., 2019]()). To date, there is sparse literature on the efficacy of *M. oleifera* wood specifically as an immobilizing matrix for fungi nor its use and ability as a Pb(II)-biosorbent. Its safety, abundance, mechanical strength, little commercial value, and ease of cultivation make it a promising biomaterial for immobilization ([Stohs and Hartman, 2015](); [Akar et al., 2007]()).

This study investigates the efficacy of *T. macrosporus* grown on *M. oleifera* wood for Pb(II) biosorption. This fungi-wood immobilized system is utilized as a biosorbent in a continuous flow column filtration system (CF) which has been studied for use in fungal biosorption ([Sağ, 2001]()). In this system, a prepared Pb(II) solution of a certain concentration is ran through the packed biosorbent that ideally traps Pb(II) ions ([Pagnanelli et al., 2009]()). The process is inexpensive, stable, accessible, and requires little energy input ([Long et al., 2019]()). Ultimately, the use of immobilized fungal biosorbents may represent a cheaper, more effective alternative to the removal of HMs such as Pb(II) from contaminated waste-water compared to traditional water treatment strategies.

2 Materials and Methods

2.1 Sample Collection and Maintenance of Fungal Cultures

Moringa oleifera wood was collected from branches of felled trees in the Ateneo de Manila University, Quezon City Philippines (14°38'16.5"N, 121°04'38.7"E). The collected wood was debarked, cut into $2 \times 2 \times 0.5$ cm pieces, boiled in dH_2O for 30 min, washed with sterile dH_2O, then dried at 70°C for 16-24h ([Akhtar et al., 2004](); [Iqbal and Saeed, 2006]()). The weight of all wood chips was measured using an analytical balance prior to their use as the immobilizing scaffold for the fungi (F). *Talaromyces macrosporus* fungal cultures used in the study were obtained from their repository at the Ateneo de Manila University ([Maini et al., 2019]()). Fungal stock cultures were maintained on potato dextrose agar (PDA, Himedia®) plate supplemented with 50 μg/mL Ampicillin (amp).

2.2 Preparation of Wood-immobilized Fungal Biosorbent

Talaromyces macrosporus spores diluted to 6.0×10^5 spores/mL in 0.1% Tween 20/Phosphate-buffered saline (PBS) were used to inoculate 60 mL of Na/P-buffered (pH 6.5) potato dextrose broth (PDB) solution containing a maximum of three dried *M. oleifera* wood (WW) pieces. The PDB was sterilized at 121°C for 15 minutes under 1.s kg/cm^2 pressure prior to the placement of WW and fungal inoculation. The PDB with the WW and the fungal inoculum was then shaken at 100 rpm, 30°C for seven days following the protocol ([Iqbal and Saeed, 2006]()). The resulting wood with fungi

was harvested via gravity filtration using Whatman (2) filter paper and dried at 70°C for 16-24h. The dry weight of the fungal biomass immobilized within the wood was determined as the weight difference of WW before and after fungal adherence. One batch of colonized wood-fungal biomass was dried in a similar manner and pulverized using an electronic grinder into $\sim 1 \times 1 \times 1$ mm pieces. Both the WW, resulting freshly colonized, and dried fungal wood matrix (WW+F) were observed at 50-300x using a Leica EZ4 Stereomicroscope and were photomicrographed after. Scale bars were added to the images using ImageJ (https://imagej.nih.gov/ij/).

2.3 Viability Test of Wood-fungal Biosorbent

Small amounts (0.10 g) of dried WW+F were placed on top of PDA plates supplemented with 50 μg/mL amp then stored at 30°C for 5 days. At the end of the incubation, the presence or absence of fungal growth was noted. These were conducted in triplicate.

2.4 Scanning Electron Microscopy

Scanning Electron Microscopy (SEM) was performed to check surface features of dried biosorbents. Oven-dried samples (60°C, 72h) measuring $\sim 1 \times 1 \times 1$ mm of F, WW, and WW+F were prepared and visualized at magnifications ranging from 100x-3000x, at Vacc = 15.0k, EC = 45.0 mA, using a Hitachi TM-1000 tabletop electron microscope.

2.5 Initial Pb(II) Contact Test (CT)

For the initial biosorption contact test, 1.2 grams of F, WW, WW+F, powdered wood (WP), and powdered wood with immobilized fungi (WP+F) were immersed in a 1000 μg/mL lead nitrate (Pb(NO$_3$)$_2$) solution (5 pH) in separate flasks and shaken at 100 rpm, 30°C for 60 minutes. All tests were performed in triplicate.

After treatment, all samples, including a control solution of unexposed 1000 μg/mL Pb(II) were gravity filtered using Whatman (2) filter paper. The supernatant containing the residual lead ions were analyzed using Inductively-Coupled Plasma Atomic Emission Spectroscopy (ICP-AES) ([Sriharsha et al., 2017](); [Iqbal and Saeed, 2006]()). The percentage of metal removed from the solution (E, %) was calculated following [Iram et al. (2015)]():

$$E = \frac{(C_i - C_f)}{C_i} \times 100 \qquad (1)$$

where E is the removal efficiency in percentage, C_i is the predetermined lead concentration (μg/mL), C_f is the final lead concentration (μg/mL).

2.6 Fourier Transform Infrared Spectroscopy

Attenuated Total Reflection-Fourier Transform Infrared Spectroscopy (ATR-FTIR) was used to identify functional groups

and vibrational frequency changes present on dried fungal biomass, and immobilized and non-immobilized wood sorbents before and after Pb(II) treatment. The IR spectra was obtained by placing 0.1 grams of the sorbent on the metal disc of the FT-IR spectrometer (PerkinElmer, Paragon 1000). Samples were analyzed in the wavenumber range of 600 to 4000 cm^{-1} at 32 scans. Spectragryph (https://www.effemm2.de/spectragryph/) was utilized in the modification and generation of the spectra images.

2.7 Continuous Flow Column Filtration Test (CF)

For the laboratory-scale Continuous Flow Column Filtration (CF) assembly, a 240 mm column setup was utilized wherein 3.0 grams of WP and/or WP+F were utilized as filters to adsorb 150 mL of 1000, 2000, and 4000 μg/mL Pb(NO$_3$)$_2$ solution that cyclically ran with a flow rate of 15 mL/min for 30 minutes. All experimental trials were done in triplicate. After the run, residual lead ions in the solution were analyzed using ICP-AES. Biosorption capacity (q) was calculated following Chen et al. (2011):

$$q = \frac{V(C_i - C_f)}{M} \qquad (2)$$

where q is the metal uptake in mg metal/g of the biosorbent or the amount of lead ions per gram of dry weight of the biosorbent, V as the volume of the metal solution in L, C$_i$ as the solution's initial Pb(II) concentration in μg/mL, C$_f$ as the solution's residual Pb(II) concentration in μg/mL, and M as the dry weight of the biosorbent in g.

2.8 Pb(II) Desorption from Biosorbent

In order to verify the Pb(II) uptake of WP+F in the CF test, desorption of Pb(II) ions was done by treating each of the biosorbents used in the set-up with 60 mL of 1.0 M Hydrochloric acid (HCl) solution shaken at 100 rpm, 25°C for 60 minutes. The sorbents were removed via gravity filtration using Whatman (2) filter paper. The supernatant containing the adsorbed Pb(II), released onto the HCl solution, was analyzed for Pb(II) concentrations via ICP-AES. Recovery in percentage, (R,%) was computed following the work of Deng et al. (2006):

$$R = \frac{M_d}{M_a} \times 100 \qquad (3)$$

where M$_d$ is the amount of Pb(II) desorbed and M$_a$ is the amount of Pb(II) adsorbed.

2.9 Statistical Analysis

Statistical analysis of the data was performed using One-Way Analysis of Variance (One-Way ANOVA) and Two-Way Analysis of Variance (Two-Way ANOVA) whenever applicable. Means were compared using Tukey's multiple comparisons test ($p < 0.05$) and Sidak's multiple comparisons

test ($p < 0.05$). Significant differences between standard deviations were determined via Brown-Forsythe ($P < 0.05$). All statistical tests were performed using GraphPad Prism (v6.01).

3 Results

3.1 Preparation of Wood-immobilized Fungal Biosorbent

Talaromyces macrosporus cells were immobilized on *M. oleifera* wood to generate and characterize the biosorbent. Representative microscopic and scanning electron micrographs of the wood before and after immobilization of fungi are presented in Figures 1 and 2B & C respectively. Whole *M. oleifera* wood from Figure 1B showed numerous open pores and interstices within xylem vessels that facilitated fungal attachment to the wood. Successful colonization of the WW is seen in Figure 1C, where fungal hyphae completely encapsulated the WW after subsequent drying at 70ºC even after grinding (Figure 1C and 2C). Microscopic examination reveals that colonization begins 48h after spore inoculation, with complete coverage after 7 days.
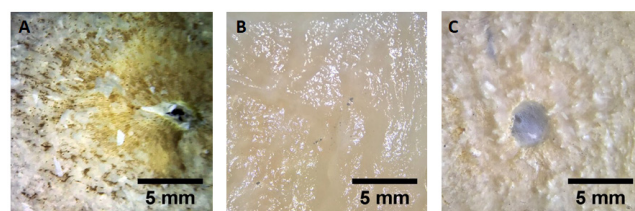

Figure 1. Various stages of the generation of the wood-immobilized fungal biosorbent. Dried uncolonized WW before immobilization of fungal hyphae (A), complete colonization after 7 days (B), dried, colonized material after 24h drying, WW+F (C).
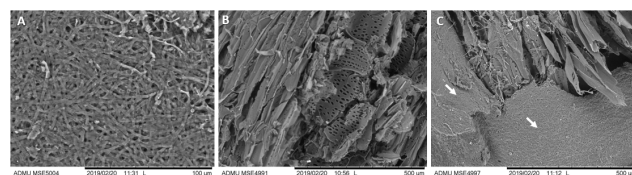

Figure 2. Surface micrographs obtained by Scanning Electron Microscopy (SEM) of (A) dried *T. macrosporus* with visible mycelia, F, 1000x (B) dried WW, 200x and (C) dried WW+F, 200x.

3.2 Initial CT

The ability of the biosorbent was determined through a contact test using 1000 μg/mL Pb(NO$_3$)$_2$. Figure 3 shows a comparison of a Pb(II)-contact test showing the removal efficiencies of WW versus WP, with and without fungal colonization. The removal efficiency of biosorbents with immobilized fungi (WW+F and WP+F) is significantly higher ($P < 0.05$)

than those with wood only (WW, WP). F had the highest contact removal of Pb(II) at 91.02% while WW had the lowest removal efficiency at 23.70%. However, removal efficiency by F is not significantly different from the removal efficiency of WP+F at 90.37% ($P < 0.05$).
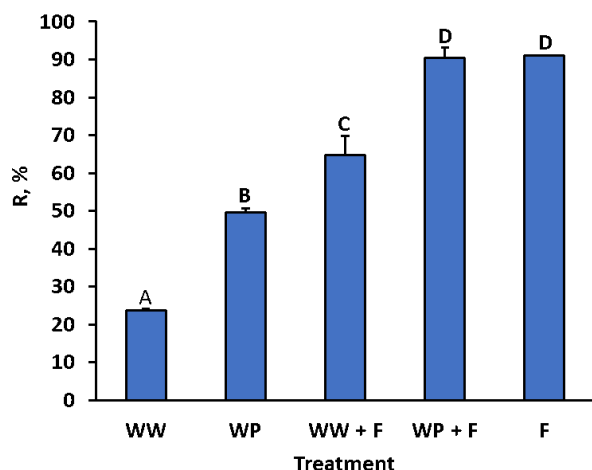

Figure 3. Pb(II) ion removal efficiency of biosorbents in contact with 1000 µg/mL Pb(II) for 60 minutes. Means that share at least one similar letter are not significantly different at Tukey's multiple comparisons test ($P < 0.05$). Assuming equal variances, Brown-Forsythe test shows that there are no significant differences between standard deviations of all test groups.

3.3 Fourier Transform Infrared Spectroscopy

Possible functional groups of fungal, wood, and wood-immobilized biomass applied in Pb(II) sorption were assessed through infrared spectroscopy seen in Figure 4. The FTIR spectra shown in Figure 5 depicts plausible Pb(II) binding sites in comparison to the biomass before and after Pb(II) treatment.

All sorbents from Figure 4 contain a broad spectral range of 3267.58 to 3338.77 cm^{-1} indicating the presence of hydroxyl (-OH) and amine (-NH) groups. Bands observed at peaks 2924.38 to 2901.65 cm^{-1} are characteristics of -CH stretching, 1743.63 to 1731.59 cm^{-1} are likely assigned to C=O stretching, 1627.03 to 1595.01 cm^{-1} are possibly related to amine groups, and peaks located at 703.33 to 663.97 cm^{-1} are assigned to C-S stretching. These frequencies were detected in all samples as shown in Table 1.

The comparison of immobilized and non-immobilized wood sorbents before and after Pb(II) treatment are shown in Tables 2 and 3. An apparent change was observed only in peak 1234 cm^{-1} (C-C, C-O, C=O stretching) of WP, which shifted into 1157.52 cm^{-1} (C-O-C antisymmetric bridge stretch) after lead binding (Table 2). For WP+F, apparent changes were only observed in peaks 1639.71 cm^{-1} (amide) and 778.65 cm^{-1} (arene), which shifted into 1631.10 cm^{-1} (amide) and none respectively (Table 4).
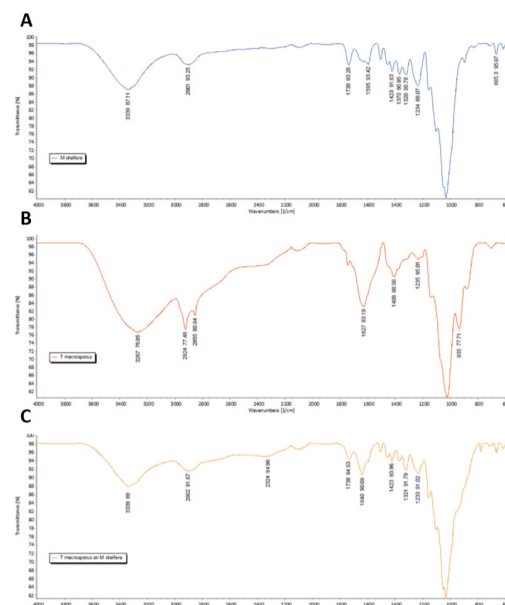

Figure 4. FTIR spectra of sorbents: WP (A) (B) dried fungi (F), and (C) dried wood immobilized with fungi (WP+F).
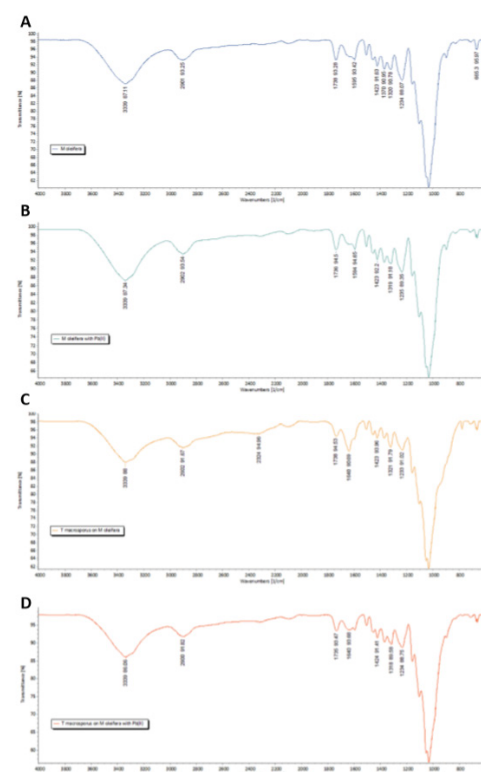

Figure 5. FTIR spectra of WP before (A) and after (B) Pb(II) treatment, and WP+F before (C) and after (D) Pb(II) treatment.

Table 1. List of possible functional groups from fungal, wood, and wood-immobilized biomass involved in Pb(II) sorption.

Biosorbent	Frequency (cm^{-1})	Functional Group
Fungi	3267.58	-OH and/or -NH
	2924.38, 2854.61	-CH stretch (Methylene)
	1743.63	C=O stretch (Alkyl carbonate)
	1627.03	N-H bend (Amine)
	1408.25	-C-O stretch
	1235.2	-C-O stretch (Ether) or -SO$_3$ stretching
	935.22	P-O-C stretch (Aromatic phosphates)
	703.33	C-S stretch (disulfide)
Wood	3339.47	-OH stretching (Alcohol)
	2902.16	-CH stretching (Methyl or methylene)
	1737.52	C=O stretching (Carboxylic acid)
	1595.01	Aromatic ring skeletal vibration (C-H, C-N, or N-H)
	1422.75	CH$_3$ bending or CH$_2$ scissoring
	1370.14	CH bending
	1234.16	C-C, C-O, or C=O symmetric stretching
	1104.21	-OH band
	897.77	CH deformation
	665.16	C-S or S-S stretch (disulfide)
Wood immobilized with fungi	3338.77	-OH stretching (Alcohol)
	2901.65	-CH stretching (Methyl or methylene)
	1731.59	C=O stretching (Carboxylic acid)
	1639.71	C=O and C-N-H stretching (Amide)
	1423.46	CH$_3$ bending or CH$_2$ scissoring
	1370.49	CH bending
	1233.01	C-C, C-O, or C=O symmetric stretching (aromatic phosphate)
	1157.47	C-O-C antisymmetric stretching
	778.65	Aromatic C-H bend
	663.97	C-S or S-S stretch (disulfide)

Table 2. Comparison of FTIR spectra between wood (WP) before and after Pb(II) sorption.

Before	After	Functional Group	Possible Assignments
3339.47	3338.63	-OH stretching (Alcohol)	Cellulose (Naumann, 2015)
2902.16	2901.16	-CH stretching (Methyl or methylene)	Cellulose (Mohaček-Grošev *et al.* 2001)
1737.52	1735.9	C=O stretching (carboxylic acid)	Xylans, hemicellulose (Traore *et al.,* 2017, Fahey *et al.* 2017)
1595.01	1593.67	Aromatic ring skeletal vibration	Lignin (Faix 1991)
1422.75	1423.09	CH$_3$ bending or CH$_2$ scissoring	Lignin and cellulose (Traore *et al.* 2017, Fahey *et al.* 2017, Faix 1991)
1370.14	1370.02	CH bending	Polysaccharides (Liang & Marchessault 1959)
1319.55	1319.07	CH$_2$ wagging	Cellulose (Liang & Marchessault, 1959)
1234.16	1157.52	From C-C, C-O, or C=O symmetric stretching to C-O-C antisymmetric stretching (Ether)	Lignin (Fahey *et al.* 2017, Liang & Marchessault, 1959)
1104.21	1104.55	-OH band	Polysaccharides (Higgins *et al.* 1961)
1032.09	1031.96	C-O stretching	Lignin, primary and secondary alcohols in cellulose, and polysaccharides (Traore *et al.* 2017)
897.77	897.76	CH deformation	Beta-glycosidic bonds in cellulose (Evans *et al.* 1992)
665.16	663.76	C-S stretch or S-S stretch (disulfide)	Disulfide bridges (cysteine) from common plant cell wall proteins (Galgoczy *et al.* 2019)

Changes in the frequencies of the wood before and after fungal immobilization are presented in Table 4. Comparison of the sorbents from Table 1 showed greater similarity in the type of functional groups between WP and WP+F than F and WP+F. Shifts in carboxylic acid (1737.52 to 1731.59 cm^{-1}), C-O-C (1104.21 to 1157.47 cm^{-1}), and aromatic CH (897.77 to 778.65 cm^{-1}) groups were observed between WP and WP+F sorbents. A major change also appeared in the band shift of 1595.01 to 1639.71 cm^{-1} suggesting a previous aromatic ring modification to an amino or carbonyl group.

3.4 CF Test

Following the results of the contact test, the residual Pb(II) ion concentration, removal efficiency, and biosorption capacity of WP versus WP+F in 1000, 2000, and 4000 μg/mL Pb(II) concentrations were tested using a CF column setup (Figure 6, 7 and 8)

Residual lead ion Pb(II) for WP and WP+F for all concentrations is summarized in Figure 6 with WP+F treatment having significantly lower (P < 0.05) residual Pb(II) concentrations than WP signifying a higher Pb(II) uptake than WP at 93, 167, and 183 μg/mL for 1000, 2000, and 4000 μg/mL respectively. WP residual Pb(II) concentration resulted to more than twice the value as the concentration also doubly increased from 1000 to 2000 μg/mL with 453 to 1323 μg/mL Pb(II) that remained and 2000 to 4000 with 1323 to 3380 μg/mL residual ions left in the solution (Figure 6E). A decreasing trend of
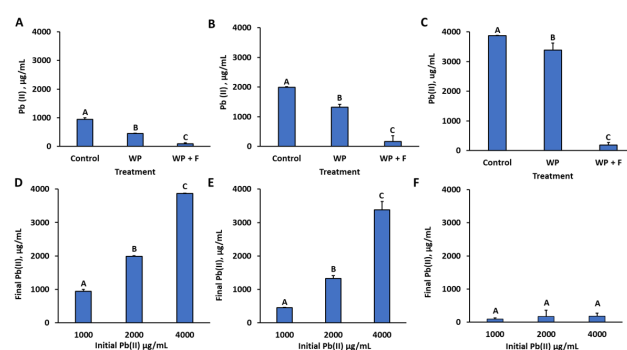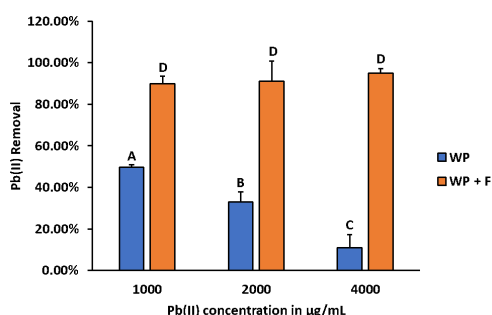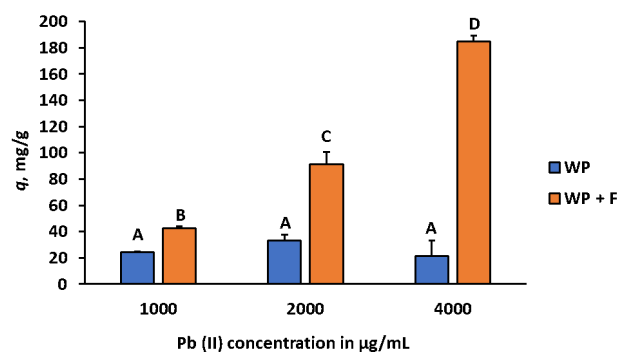

Figure 6. Residual Pb(II) ion concentration of biosorbents (WP, WP+F) in contact with 1000 (A), 2000 (B), and 4000 μg/mL Pb(II) (C) for 30 minutes in assembled CF system. Comparison of residual Pb(II) ion concentration of control (D), WP (E), and WP+F (F) in 1000, 2000, and 4000 μg/mL Pb(II) concentrations. Means that share at least one similar letter are not significantly different at Tukey's multiple comparisons test (P < 0.05). Bars indicate standard deviation of at least three replicates.

Table 3. Comparison of FTIR spectra between wood immobilized with fungi (WP+F) before and after Pb(II) sorption.

Before	After	Functional Group	Possible Assignments
3338.77	3338.79	-OH stretching (Alcohol)	Cellulose (plant) or chitin (fungi) (Naumann, 2015)
2901.65	2901.64	-CH stretching (Methyl or methylene)	Cellulose (plant) or chitin (fungi) (Naumann, 2015)
1731.59	1734.84	C=O stretching (carboxylic acid)	Xylans, hemicellulose, mannan (Naumann, 2015)
1639.71	1631.1	C=O and C-N-H stretching (amide)	Chitin amide (Naumann, 2015)
1423.46	1423.63	CH_3 bending or CH_2 scissoring	Lignin and cellulose (Naumann, 2015)
1370.49	1369.91	CH bending	Polysaccharides (Naumann, 2015)
1233.01	1234.02	C-C, C-O, or C=O symmetric stretching	Lignin (Fahey *et al.* 2017)
1157.47	1158.29	C-O-C antisymmetric stretching (ether)	Polysaccharides (Fahey *et al.* 2017, Liang & Marchessault 1959)
778.65	-	From aromatic CH bend to apparent loss of functionality	Lignin fragments (guaiacyl) and beta-galactosyl residues (Fahey *et al.* 2017)
663.97	663.61	C-S stretch or S-S stretch (disulfide)	Disulfide bridges (Galgoczy *et al.* 2019)

Table 4. Comparison of FTIR spectra between wood (WP) before and after fungal colonization (WP+F).

Before	After	Functional Group	Possible Assignments
3339.47	3338.77	-OH stretching (Alcohol)	Cellulose (plant) or chitin (fungi) (Naumann, 2015)
2902.16	2901.65	-CH stretching (Methyl or methylene)	Cellulose (plant) or chitin (fungi) (Naumann, 2015)
1737.52	1731.59	C=O stretching (carboxylic acid)	Xylans, hemicellulose, mannan (Naumann, 2015)
1595.01	1639.71	From aromatic ring skeletal vibration (lignols) to C=O and C-N-H stretching (amide)	Chitin amide (Naumann, 2015)
1422.75	1423.46	CH_3 bending or CH_2 scissoring	Lignin and cellulose (Traore *et al.* 2018, Naumann, 2015)
1370.14	1370.49	CH bending	Polysaccharides (Liang & Marchessault 1959)
1234.16	1233.01	C-C, C-O, or C=O symmetric stretching	Lignin (Liang & Marchessault, 1959)
1104.21	1157.47	C-O-C antisymmetric stretching (Ether)	Polysaccharides (Fahey *et al.* 2017, Liang & Marchessault, 1959)
897.77	778.65	Aromatic CH bend	Lignin fragments (guaiacyl) and beta-galactosyl residues (Fahey *et al.* 2017)
665.16	663.97	C-S stretch or S-S stretch (disulfide)	Disulfide bridges (Galgoczy *et al.* 2019)

Figure 7. Pb(II) ion removal efficiency (%) of biosorbents (WP, WP+F) in contact with 1000, 2000, and 4000 µg/mL Pb(II) for 30 minutes in assembled CF system. Means that share at least one similar letter are not significantly different at Tukey's multiple comparisons test (P < 0.05). Bars indicate standard deviation of at least three replicates.

Figure 8. Biosorption capacity (*q*) of biosorbents (WP, WP+F) in contact with 1000, 2000, and 4000 µg/mL Pb(II) for 30 minutes in assembled CF system. Two-way ANOVA shows that means are statistically significantly different at P < 0.05. Means that share at least one similar letter are not significantly different at Tukey's multiple comparisons test (P < 0.05). Bars indicate standard deviation of at least three replicates.

the removal efficiency of WP tested in increasing Pb(II) concentrations presented in Figure 7 is congruent to these results. However, the residual ion concentration of WP+F is not significantly different at different Pb(II) concentrations at $P < 0.05$ (Figure 6F). This is similarly represented in Figure 7, where the removal efficiency of WP+F remained statistically insignificant at 90-95%, unaffected by initial Pb(II) concentration.

The biosorption capacity (q) of WP+F significantly increases from 42.67 to 91.13, and from 92.3 to 184.83 as Pb(II) concentration increases from 1000 ppm to 2000 ppm and from 2000 ppm to 4000 ppm respectively (Figure 8). The q of WP+F was also found to be significantly higher than that of WP at $P < 0.05$, with the latter having an insignificantly different q for the same biosorbent groups regardless of initial Pb(II) concentration.

A comparison of the residual Pb(II) concentrations for the contact test and the CF test is shown below in Figure 9. There are no significant differences between the contact test and CF results at $P < 0.05$ for WP and WP+F.
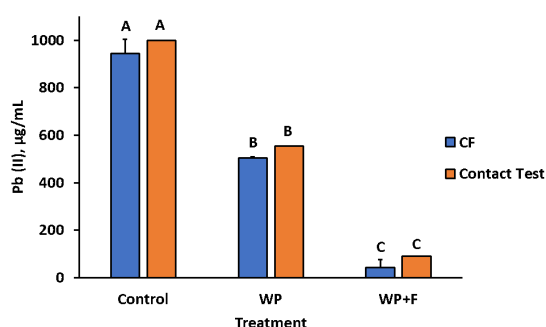
Table 5. Fungal weight in immobilized biosorbent in grams (g). The average weight increase by fungal colonization was 0.16 ± 0.016.

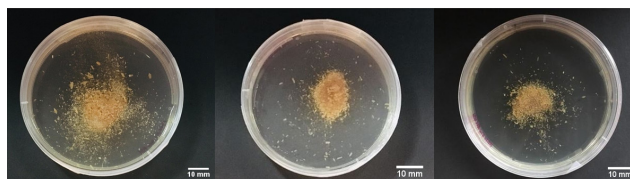| Dried Wood (WW) (g)	Dried Colonized (WW+F) (g)	Fungal Weight (g)
1.20 ± 0.002	1.40 ± 0.010	0.20 ± 0.010
1.25 ± 0.002	1.42 ± 0.009	0.17 ± 0.020
1.25 ± 0.003	1.43 ± 0.010	0.18 ± 0.020
0.94 ± 0.010	1.04 ± 0.021	0.10 ± 0.020
0.91 ± 0.012	1.05 ± 0.022	0.14 ± 0.010

Figure 10. Triplicate viability test of WP+F tested on PDA plates supplemented with 50 μg/mL amp. Photographs were taken after 5 days of incubation at 30°C.
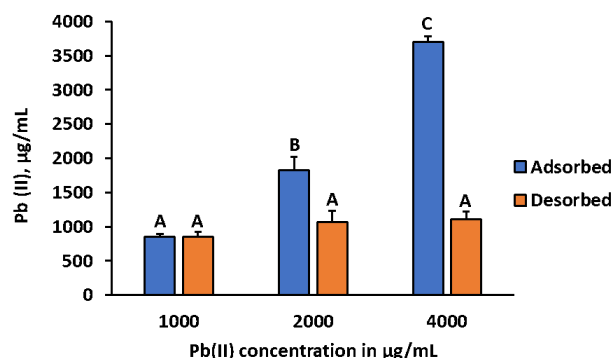

Figure 9. Comparison of Contact test and CF residual Pb(II) ion concentration by biosorbents in contact with 1000 μg/mL Pb(II). Means that share at least one similar letter are not significantly different at Tukey's multiple comparisons test ($P < 0.05$). Assuming equal variances, Sidak's multiple comparisons test shows that there are no significant differences between computed (Contact Test) and actual values (CF) of all test groups.

T. macrosporus immobilized in wood was shown to yield an average of 0.16 ± 0.016 grams from Table 5. Furthermore, preparation of the powdered wood-fungal biosorbent did not exhibit fungal growth after 4 days of incubation from Figure 10.

3.5 Pb(II) Desorption from WP+F Biosorbent

Amounts of Pb(II) desorbed and recovery percentage of the powdered wood-fungal biosorbent (WP+F) are shown in Figures 11 and 12.

Desorption of the Pb(II) ions from WP+F biomass in contact with all concentrations was not significantly different

Figure 11. Comparison of adsorbed and desorbed Pb(II) ions of utilized WP+F biosorbents in CF test for concentrations of 1000, 2000, and 4000 μg/mL. Two-way ANOVA shows that means are statistically significantly different at $P < 0.05$. Means that share at least one similar letter are not significantly different at Tukey's multiple comparisons test ($P < 0.05$). Bars indicate standard deviation of at least three replicates.
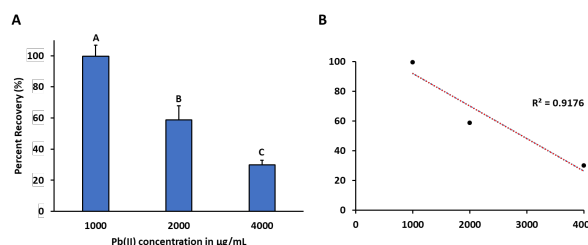

Figure 12. Percent recovery (%) of WP+F biosorbents from CF set-up in contact with 1000, 2000, and 4000 μg/mL Pb(II) solutions after treatment with 1.0 M HCl for 60 minutes. One-way ANOVA shows that means are statistically significantly different at $P < 0.05$. Bars indicate standard deviation of at least three replicates (A). A linear regression model produced an R^2 value of 0.9176 to express the relationship between the data points (B).

(P < 0.05) from the Pb(II) ions adsorbed at 1000 µg/mL as presented in Figure 11. However, it is important to note that most of the Pb(II) ions adsorbed by the biomass at 1000 µg/mL were recovered at 99.61% shown in Figure 12. From the same figure, an almost linear decrease of the recovery percentage was shown as the Pb(II) ion concentration doubles from 99.61% to 58.71% for 1000 to 2000 µg/mL and 58% to 30.02% for 2000 to 4000 µg/mL. This trend is supported by the regression model which produced an R^2 value of 0.9176 indicating a large positive linear association.

4 Discussion

4.1 Preparation of Wood-immobilized Fungal Biosorbent and SEM Analysis

Fungal colonization of the prepared biosorbent produced similar results to the study using *Carica papaya* softwood (Iqbal and Saeed, 2006). The growth of *T. macrosporus* mycelia along the surface of *M. oleifera* wood as shown in Figure 1C presented a uniform distribution. This allows for a greater number of open binding sites, and exposure of a wider surface area for HM binding (Ding et al., 2019). This represents one of the advantages of immobilized systems over free cell suspension cultures where the latter is tightly clumped resulting in diffusional restrictions and lower surface area of adsorption (Ramrakhiani et al., 2016; Iqbal and Edyvean, 2004).

The entrapment of *T. macrosporus* mycelia on *M. oleifera* wood in a relatively short time span of seven days indicates the efficiency in generating the biosorbent without prior chemical treatment. This is in contrast with several other modes of immobilization that are costly, laborious, and require sophisticated equipment (Iqbal and Saeed, 2006). This also addresses common operative obstacles found in the preparation of most immobilizing materials such as their poor mechanical strength, restrictive diffusion capacities, and lack of open spaces to accommodate active cell growth (Sriharsha et al., 2017; Li et al., 2008).

4.2 Initial CT

The Pb(II) removal efficiency of *T. macrosporus* is highlighted in Figure 3 where the removal percentage of F (91.02%), WW+F (64.81%), and WP+F (90.37%) are significantly higher than that of WW (23.70%) and WP (49.63%). These findings are in line with studies wherein immobilants colonized with fungi removed more heavy metals in solution than the immobilant alone (Sriharsha et al., 2017; Zahmatkesh et al., 2018; Iqbal and Saeed, 2006). This may be due to the sheer number of complex fungal polysaccharide residues such as chitin and glucan, which are found to be more abundant in available binding sites compared to other plant polysaccharides such

as cellulose and lignin (Ge and Li, 2018; Shakya et al., 2016).

However, the Pb(II) removal efficiency between F and WP+F were not significantly different from each other despite the lower fungal biomass component of WP+F (0.16 ± 0.016 g) compared to F (1.20 ± 0.006 g) as seen in Table 5. This finding differs from the studies of Ding et al. (2019), Sriharsha et al. (2017), Ramrakhiani et al. (2016), and Iqbal & Saeed (2006) wherein their immobilized system biosorbents had a significantly higher removal efficiency than fungi alone. This may indicate an inherent strength of polarity and abundance of effective binding sites found on the fungal cell wall even at low amounts of fungal biomass (Ge and Li, 2018).

Aside from functional group abundance and availability, it has also been suggested that fungal colonization of wood has biochemical impacts on the structure of plant cell walls, enhancing HM binding capacity (Saravanan and Ravikumar, 2015). Certain Ascomycete enzymes such as lignin peroxidase, hemicellulase, laccase, phenol oxidase, cellobiose dehydrogenase, beta-glucosidase, and cellulase (Janusz et al., 2017; Goyari et al., 2015), can cleave the covalent linkages between lignin, cellulose, hemicellulose, pectin, and other polysaccharide components of lignocellulose, increasing the number, distribution, exposure, and polarity of metal-affinitive functional groups in wood tissue (Zhao et al., 2018).

4.3 FTIR Analysis

The FTIR spectra of dried fungal biomass, wood immobilized, and non-immobilized sorbents from Figure 4 were analyzed to list and verify possible sorbent-metal ion binding sites in Pb(II) removal. FTIR has previously been used to identify potential sorption sites for Pb(II) in fungal biomass (Aytar et al., 2014), various wood and cellulosic tissues (Traoré et al., 2017; Fahey et al., 2017; Malik et al., 2016), and wood derived materials (Putra et al., 2014).

Dried fungal biomass has been documented to possess hydroxyl, amino, and carboxyl groups from N-acetylglucosamine as components of their chitinous cell walls which have been proven to bind to Pb(II) ions (Long et al., 2019; Sriharsha et al., 2017; Gube, 2016). Similarly, sulfhydryl (Akar et al., 2007) and carbonyl groups (Aytar et al., 2014) have been also documented in Pb(II) binding. Results from Table 1 confirm the presence of several functional groups common to other Ascomycetes capable of Pb(II) sorption (Long et al., 2019).

Similar to fungal biomass, the use of cellulosic materials in the removal of various heavy metals including Pb(II) has been described and summarized extensively (Malik et al., 2016). Cellulosic, hemicellulosic, and lignin components from wood sorbents may contain hydroxyl, amino, aromatic, and carbonyl groups responsible for HM binding (Putra et al., 2014). These components were detected in WW, WP,

WW+F, and WP+F, presented in Table 1.

Comparing the IR spectra of the sorbents before and after Pb(II) exposure shown in Tables 2 and Table 3 indicate minimal peak shifts within -OH (3339.47 to 3338.63 cm^{-1}), CH (2902.16 to 2901.16 cm^{-1}), and C-S and S-S (665.16 to 663.76 cm^{-1}), and a major change in the vibration band intensities of the binding sites at 1234.15 to 1157.52 cm^{-1} (from C=O to C-O-C) for WP, and 1639.71 to 1631.10 cm^{-1} (C=O and C-N-H) and 778.65 cm^{-1} to none (aromatic CH) for WP+F.

The shift of the peak intensity from 1234.15 to 1157.52 cm^{-1} in WP (Table 2) may indicate binding of Pb(II) to C=O groups in lignin which forms a more stable complex leading to a lower C=O peak intensity; this may also refer to the exposure of more C-O-C groups that constitute other lignin components and glycosidic linkages (Njoki et al., 2016). For WP+F (Table 3), the shift of the peak intensity from 1639.71 to 1631.10 cm^{-1} may indicate binding of Pb(II) towards the electronegative oxygen or nitrogen group, while the loss of peak intensity from 778.65 cm^{-1} may indicate Pb(II) capture by arenes which form less reactive organometallic complexes (Yang et al., 2018). Minimal and apparent shifts in peak intensities observed in both WP and WP+F after Pb(II) sorption (Table 2, 3) confirm the possible involvement of hydroxyl, carboxyl, amine, and aromatic groups in the adsorption process following Pb(II) exposure as described in literature (Aytar et al., 2014).

Furthermore, apparent shifts in peak intensities can be observed within 1595.01 to 1639.71 cm^{-1} (lignol to amide), 1104.21 to 1157.47 cm^{-1} (ether), and 897.77 to 778.65 (CH deformation into arene) in wood after fungal colonization (Table 4). These suggest chemical changes or rearrangements in the plant cell wall components following fungal enzymatic attack (Cui et al., 2017). For instance, the peak shift from 1595.01 to 1639.71 cm^{-1} (lignol to amide) may be due to the cross-linking of fungal cell wall proteins with galactosyl residues on lignin thereby forming a chitin amide (Naumann et al., 2005). The peak shift from 897.77 to 778.65 cm^{-1} (CH deformation into arenes) which, following Fahey et al. (2017), is assigned to the formation of beta galactosyl residues and lignol units, indicating cleavage of lignocellulose into simpler chemical units by fungal interaction (Chen et al., 2011).These suggested chemical changes on the plant cell wall by fungal interaction may have affected biosorption capacity and Pb(II) removal by the WP+F biosorbent, another possible explanation as to why WP+F has no significant difference in biosorption capacity compared to F, but has significantly more Pb(II) sorption compared to WW and WP at P < 0.05.

4.4   CF Tests

Following the results of the Pb(II) contact test, the Pb(II) biosorption capacities (q) of WP and WP+F in a CF setup

were investigated. The sorption of WP+F Pb(II) was found to be higher compared to WP (Figures 6-8), with q values for WP+F growing concomitant to increasing Pb(II) concentrations (Figure 8) similar to the work of Long et al. (2019), Akar et al. (2005), and Say et al. (2003a,b). This may be primarily attributed to the inherently high amounts of chitin and other heavily glycosylated substances found on the fungal cell wall which are widely documented for their functionality in stable, high-capacity Pb(II) binding and complexation (Ayangbenro and Babalola, 2017; Dhankhar and Hooda, 2011). These binding site characteristics coupled with elevated metal concentrations favors high mass transfer which drives sorbent-metal collisions that ultimately increase sorption (Fan et al., 2008).

On the other hand, q values for WP which have no significant differences (P > 0.05) despite increasing initial Pb(II) concentrations (Figure 8). This may indicate a limitation in the number and/or distribution of Pb(II)-affinitive sites for WP. This is not surprising since plant cellulose and lignocellulose, while having HM-binding sites, have been reported to have poor application for metal adsorption due to their tightly closed crystalline chemical structure that decreases the number and availability of exposed HM-binding sites (Morin-Crini et al., 2018).

Despite the lower q values for WP, values ranging from 21.17 - 33.33 mg/g are still higher than most other *M. oleifera* components tested in Pb(II) biosorption studies, such as the bark, fruit, leaf and seed (Basra et al., 2014; Obuseng et al., 2012; Reddy et al., 2010; Mataka et al., 2006). The differences in the ratios of lignin, cellulose, and hemicellulose on the cell wall of different plant tissues can influence the density, polarity, number, and distribution of metal-affinitive functional groups such as hydroxyl, carbonyl, and sulfhydryl (Chen et al., 2011). Both sapwood and heartwood generally have a higher overall lignin-cellulose-hemicellulose ratio than leaves, roots, or bark which may explain the greater sorption capacities for *M. oleifera* softwood measured in this work (Morin-Crini et al., 2018; Jin et al., 2012).

Comparing q values between the CF test and the immobilant-free CT at 1000 μg/mL (Figure 9), it can be seen that there was no significant difference between the treatments (P < 0.05), indicating that application of the biosorbent in a spatially different setup such as a column filtration system does not significantly change its ability to remediate Pb(II) at 1000 μg/mL. This suggests that the biosorbent is stable for use in a column system with continuous flow of contaminated wastewater at the parameters tested in this work, making it ideal for industrial application. Moreover, the preparation as a non-living biomass (Figure 10) confers usage advantages such as its inability to change fungal cell surface structures and/or secrete extrolites which can affect its efficacy as a biosorbent over time. The WP+F set up shows no further growth after

drying, an important consideration for its application and use.

4.5 Pb(II) Desorption from WP+F Biosorbent

To verify the Pb(II) ions adsorbed by the biomass in the assembled CF set-up and determine its potential reusability in Pb(II) ion recycling processes after water treatment, the amount of Pb(II) ions should be readily desorbed under suitable conditions. The recovery of the Pb(II) ions was not significantly different at $P < 0.05$ regardless of concentrations (Figure 11). However, the highest recovery percentage of 99.61% from the biosorbent was found in contact with 1000 μg/mL (Figure 12) but decreased almost linearly when desorption using 1.0M of HCl is performed at 2000 μg/mL and 4000 μg/mL treatment groups (Figure 12B).

To fully desorb the Pb(II) ions at 2000 and 4000 μg/mL, HCl concentrations may need to be increased to recover the equivalent amount of Pb(II) ions adsorbed from the biomass since the degree of desorption activity is dependent on the ratio between the desorbing eluent (liquid phase) and the sorbent-sorbate complex (solid phase) (Chatterjee and Abraham, 2019). This is supported by the studies of Kariuki et al. (2016), and Akhtar et al. (2004) wherein increasing concentrations of HCl enhances the desorption capacity of HM in higher HM concentrations. However, higher concentrations of HCl can degrade immobilized biological tissues leading to a loss in biomass and biosorption capacity which can drastically decrease the biosorbent's degree of reusability for repeated use (Hammaini et al., 2007).

5 Conclusion

Moringa oleifera proved to be a suitable substrate for the immobilization of *T. macrosporus* and the generation of fungiwood biosorbents which successfully adsorbed Pb(II) at 1000, 2000, and 4000 ug/mL, as measured through ICP-AES. Minimal amounts (0. 0.16 ± 0.016 g) of *T. macrosporus* colonizing the wood (WP+F) was enough to remove 91-95% of Pb(II) in the test solutions and significantly increase its biosorption capacity for all Pb(II) concentrations in 30 minutes. The sorptive ability of non-immobilized fungal biomass (F) and WP+F were found to be similar, but the latter is more efficient for greater biomass generation. Powdered biomass (WP and WP+F) act as significantly better biosorbents for Pb(II) binding compared to whole (WW, WW+F). The significantly higher and continued Pb(II) uptake of WP+F compared to WP regardless of starting metal concentration may be attributed to the unsaturation or difference in the number, type, and distribution of binding sites in the fungal and/or plant cell walls exposed to the metal fraction, as suggested by previous studies. FTIR Analysis showed hydroxyl, carboxyl, amine, and aromatic groups which may participate in the Pb(II) sorption process. The resulting Pb(II) uptake of WP+F from the contact test identical to the removal in the CF setup shows that the biosorbent can be used for both a CF and open system without compromising adsorption ability. The recovery of Pb(II) from acid treated biosorbent proves Pb(II) entrapment in the WP+F matrix, being able to trap as much as 99.61% of all available ions in the aqueous solution. The results of this work can be considered for potential applications and design of biotreatment methodologies for Pb(II)-contaminated wastewaters.

Author Contributions

ZAN Maini is the project leader who was responsible for overseeing the entire work, drafting the manuscript and assisting in all the experiments performed. NTB Flores and EP Muñoz were responsible for performing all experiments found in the study. Additionally, NTB Flores was primarily responsible for the statistical analysis, while EP Muñoz was primarily responsible for sample collection and preparation of the biosorbent.

Acknowledgements

Conflict of Interest Declaration

The authors have no conflict of interest in the research reported here.

References

Ahluwalia, S.S. and Goyal, D., 2007. Microbial and plant derived biomass for removal of heavy metals from wastewater. Bioresource Technology, 98(2007), 2243-2257. https://doi.org/10.1016/j.biortech.2005.12.006

Akar T, Tunali S and Cabuk A., 2007. Study on the Characterization of Lead (II) Biosorption by Fungus Aspergillus parasiticus. Applied Biochemistry and Biotechnology, 136, 389-406. https://doi.org/10.1007/s12010-007-9032-8

Akar, T., Tunali, S. and Kiran, I., 2005. Botrytis cinereal as a new fungal biosorbent for removal of Pb(II) from aqueous solutions. Biochemical Engineering Journal, 25(3), 227-235. https://doi.org/10.1016/j.bej.2005.05.006

Akhtar, N., Iqbal, J. and Iqbal, M., 2004. Removal and recovery of nickel (II) from aqueous solution by loofa sponge-immobilized biomass of Chlorella sorokiniana: characterization studies. Journal of Hazardous Materials, 85-94.
https://doi.org/10.1016/j.jhazmat.2004.01.002

Anwar, F., Latif, S., Ashraf, M. and Gilani, A.H., 2007. *Moringa oleifera*: a food plant with multiple medicinal uses. Phytotherapy Research, 21, 17-25.
https://doi.org/10.1002/ptr.2023

Assi, M.A., Hezmee, M.N., Haron, A.W., Sabri, M.Y. and Rajion, M.A., 2016. The detrimental effects of lead on human and animal health. Veterinary World, 9(6), 660-671.
https://doi.org/10.14202/vetworld.2016.660-671

Ayangbenro, A.S., and Babalola, O.O., 2017. A new strategy for heavy metal polluted environments: A review of microbial biosorbents. International Journal of Environmental Research and Public Health, 14(1), 1-16.
https://doi.org/10.3390/ijerph14010094

Aytar, P., Gedikli, S., Buruk, Y., Cabuk, A. and Burnak, N., 2014. Lead and nickel biosorption with a fungal biomass isolated from metal mine drainage: Box-Behnken experimental design. International Journal of Environmental Science and Technology, 11(6), 1631-1640.
https://doi.org/10.1007/s13762-013-0354-5

Basra, S., Iqbal, Z., Rehman, K., Rehman, H. and Ejaz, M.F., 2014. Time course changes in pH, electrical conductivity and heavy metals (Pb, Cr) of wastewater using *Moringa oleifera* Lam. Seed and alum, a comparative evaluation. Journal of Applied Research and Technology, 12(3), 560-567.
https://doi.org/10.1016/S1665-6423(14)71635-9

Cai, C.X., Xu, J., Deng, N.F., Dong, X.W., Tang, H., Liang, Y., Fan, X.W. and Li, Y.Z., 2016. A novel approach of utilization of the fungal conidia biomass to remove heavy metals from the aqueous solution through immobilization. Scientific Reports, 6(36546), 1-12.
https://doi.org/10.1038/srep36546

Chatterjee, A. and Abraham, J., 2019. Desorption of heavy metals from metal loaded sorbents and e-wastes: A review. Biotechnology Letters, 41(3), 319-333.
https://doi.org/10.1007/s10529-019-02650-0

Chen, B., Yuan, M., and Liu, H., 2011. Removal of polycyclic aromatic hydrocarbons from aqueous solution using plant residue materials as a biosorbent. Journal of Hazardous Materials, 188(1-3), 436-442.
https://doi.org/10.1016/j.jhazmat.2011.01.114

Cui, H., Li, F., Ren, B., Xue, C., Cui, C., and Wang, J., 2017. Biosorption of aquatic Pb2, Hg2, and Cd2 using a combined biosorbent - Aspergillus niger-Treated Rice Straw. Separation Science and Technology, 53(4), 626-635.
https://doi.org/10.1080/01496395.2017.1412463

Das, M., and Adholeya, A., 2015. Potential Uses of Immobilized Bacteria, Fungi, Algae, and Their Aggregates for Treatment of Organic and Inorganic Pollutants in Wastewater. ACS Symposium Series Water Challenges and Solutions on a Global Scale, 319-337.
https://doi.org/10.1021/bk-2015-1206.ch015

Deng, L., Su, Y., Su, H., Wang, X., and Zhu, X., 2006. Biosorption of copper (II) and lead (II) from aqueous solutions by nonliving green algae Cladophora fascicularis: Equilibrium, kinetics and environmental effects. Adsorption,12(4), 267-277.
https://doi.org/10.1007/s10450-006-0503-y

Dhankhar, R. and Hooda, A., 2011. Fungal biosorption - an alternative to meet the challenges of heavy metal pollution in aqueous solutions. Environmental Technology, 32(5), 467-491.
https://doi.org/10.1080/09593330.2011.572922

Ding, H., Luo, X., Zhang, X. and Yang, H., 2019. Alginate-immobilized Aspergillus niger: Characterization and biosorption removal of thorium ions from radioactive wastewater. Colloids and Surfaces A: Physicochemical and Engineering Aspects, 562, 186-195.
https://doi.org/10.1016/j.colsurfa.2018.11.032.

Evans, P., Michell, A. and Schmalzl, K., 1992. Studies of the degradation and protection of wood surfaces. Wood Science and Technology,26(2), 151-163.
https://doi.org/10.1007/bf00194471

Fahey, L.M., Nieuwoudt, M.K. and Harris, P.J., 2017. Predicting the cell-wall compositions of Pinus radiata (radiata pine) wood using ATR and transmission FTIR spectroscopies. Cellulose, 24(12), 5275-5293.
https://doi.org/10.1007/s10570-017-1506-4

Faix, O., 1991. Classification of Lignins from Different Botanical Origins by FT-IR Spectroscopy. Holzforschung, 45(S1), 21-28.
https://doi.org/10.1515/hfsg.1991.45.s1.21

Fan, T., Liu, Y., Feng, B., Zeng, G., Yang, C., Zhou, M. and Wang, X., 2008. Biosorption of cadmium(II), zinc(II) and lead(II) by Penicillium simplicissimum: Isotherms, kinetics and thermodynamics. Journal of Hazardous Materials, 160(2-3), 655-661.
https://doi.org/10.1016/j.jhazmat.2008.03.038.

Galgoczy, L., Yap, A., and Marx, F., 2019. Cysteine-Rich Antifungal Proteins from Filamentous Fungi are Promising Bioactive Natural Compounds in Anti-Candida Therapy. Israel Journal of Chemistry, 59(5), 360-370.
https://doi.org/10.1002/ijch.201800168

Ge, Y. and Li, Z., 2018. Application of Lignin and Its Derivatives in Adsorption of Heavy Metal Ions in Water: A Review. ACS Sustainable Chemistry and Engineering, 6(5), 7181-7192.
https://doi.org/10.1021/acssuschemeng.8b01345

Goyari, S., Devi, S., Bengyella, L., Khan, M., Sharma, C.K., Kalita, M.C., and Talukdar, N.C., 2015. Unveiling the optimal parameters for cellulolytic characteristics of Talaromyces verruculosus SGMNPf3 and its secretory enzymes. Journal of Applied Microbiology, 119(1), 88-98.
https://doi.org/10.1111/jam.12816

Gube, M., 2016. Fungal Molecular Response to Heavy Metal Stress. In: Esser, K., Hoffmeister, D. (eds) Biochemistry and Molecular Biology. The Mycota (A Comprehensive Treatise on Fungi as Experimental Systems for Basic and Applied Research) vol III (pp. 47-68), Cham, Switzerland: Springer.
https://doi.org/10.1007/978-3-319-27790-5_4

Hammaini, A., Gonzales, F., Ballester, A., Blazquez M.L. and Munoz, J.A., 2007. Biosorption of heavy metals by activated sludge and their desorption characteristics. Journal of environmental Management, 84, 419-426.
https://doi.org/10.1016/j.jenvman.2006.06.015

Hauptman, M., Bruccoleri, R. and Woolf, A.D., 2017. An Update on Childhood Lead Poisoning. Clinical Pediatric Emergency Medicine, 18(3), 181-192.
https://doi.org/10.1016/j.cpem.2017.07.010.

Higgins, H.G., Stewart, C.M., and Harrington, K.J., 1961. Infrared spectra of cellulose and related polysaccharides. Journal of Polymer Science, 51(1), 59-84. https://doi.org/10.1002/pol.1961.120510105

Iqbal, M. and Edyvean, R.G., 2004. Biosorption of lead, copper and zinc ions on loofa sponge immobilized biomass of Phanerochaete chrysosporium. Minerals Engineering, 17, 217-223. https://doi.org/10.1016/j.mineng.2003.08.014

Iqbal, M. and Saeed, A., 2006. Entrapment of fungal hyphae in structural fibrous network of papaya wood to produce a unique biosorbent for the removal of heavy metals. Enzyme and Microbial Technology, 39, 996-1001. https://doi.org/10.1016?j.enzmictec.2006.02.019

Iram, S., Shabbir, R., Zafar, H., and Javaid, M., 2015. Biosorption and Bioaccumulation of Copper and Lead by Heavy Metal-Resistant Fungal Isolates. Arabian Journal for Science and Engineering, 40(7), 1867-1873. https://doi.org/10.1007/s13369-015-1702-1

Janusz, G., Pawlik, A., Sulej, J., Swiderska-Burek, U., Jarosz-Wilkolazka, A. and Paszczynski, A., 2017. Lignin degradation: microorganisms, enzymes involved, genomes analysis and evolution. FEMS Microbiology Reviews, 41(6), 941-962. https://doi.org/10.1093/femsre/fux049

Jha, S., Chauhan, R. and Dikshit, S.N., 2014. Fungal biomass as biosorbent for removal of heavy metal from industrial wastewater effluent. Asian Journal of Plant Sciences, 13(2), 93-97. https://doi.org/10.3923/ajps.2014.93.97

Jin, W.J., Singh, K., Zondlo, J., Wang, J.X. and Brar, J., 2012. Pyrolysis kinetics of physical components of wood and wood-polymers using isoconversion method. Agriculture, 3, 12-32. https://doi.org/10.3390/agriculture3010012

Kapoor, A. and Viraraghavan, T., 1995. Fungal biosorption - an alternative treatment option for heavy metal bearing wastewaters: A review. Bioresource Technology, 53(1995), 195-206. https://doi.org/10.1016/0960-8524(95)00072-M

Kariuki, Z., Kiptoo, J. and Onyancha, D., 2016. Biosorption of lead and copper using rogers mushroom biomass 'Lepiota hystrix'. South African Journal of Chemical Engineering, 23, 62-70. https://doi.org/10.1016/j.sajce.2017.02.001

Li, X., Liao, D., Xu, X., Yang, Q., Zeng, G., Zheng, W., and Guo, L., 2008. Kinetic studies for the biosorption of lead and copper ions by Penicillium simplicissimum immobilized within loofa sponge. Journal of Hazardous Materials, 159(2-3), 610-615. https://doi.org/10.1016/j.jhazmat.2008.02.068

Liang, C. Y., and Marchessault, R. H., 1959. Infrared spectra of crystalline polysaccharides. II. Native celluloses in the region from 640 to 1700 cm.1. Journal of Polymer Science, 39(135), 269-278. https://doi.org/10.1002/pol.1959.1203913521

Long, J., Yuvaraja, G., Zhou, S., Mo, J., Li, H., Luo, D.. and Reddy, G. M, 2019. Inactive Fusarium Fungal strains (ZSY and MJY) isolation and application for the removal of Pb(II) ions from aqueous environment. Journal of Industrial and Engineering Chemistry, 72, 442-452. https://doi.org/10.1016/j.jiec.2018.12.047

Maini, Z.A.N., Aribal, K.M., Narag, R.M., Melad, J.K.L., Frejas, J.A., Arriola, L.A., Gulpeo, P.C., I.A. and Lopez, C., 2019. Lead (II) tolerance and uptake capacities of fungi isolated from a polluted tributary in the Philippines. Applied Environmental Biotechnology, 4(1), 18-29. https://doi.org/10.26789/AEB.2019.01.004

Malik, D.S., Jain, C.K., and Yadav, A.K., 2016. Removal of heavy metals from emerging cellulosic low-cost adsorbents: A review. Applied Water Science, 7(5), 2113-2136. https://doi.org/10.1007/s13201-016-0401-8

Mataka, L.M., Henry, E.M., Masamba, W.R. and Sajidu, S.M., 2006. Lead remediation of contaminated water using Moringa stenopetala and *Moringa oleifera* seed powder. International Journal of Environmental Science and Technology, 3(2), 131-139. https://doi.org/10.1007/bf03325916

Michalak, I., Chojnacka, K. and Krowiak, AW., 2013. State of the art for the biosorption process - a review. Applied Biochemistry and Biotechnology, 170, 1389-1416. https://doi.org/10.1007/s12010-013-0269-0

Mirzabeygi, M., Abbasnia, A., Yunesian, M., Nodehi, RN., Yousefi, N., Hadi, M. and Mahvi, AH., 2017. Heavy metal contamination and health risk assessment in drinking water of Sistan and Baluchistan, Southeastern Iran. Human and Ecological Risk Assessment: An International Journal, 23(8), 1893-1905. https://doi.org/10.1080/10807039.2017.1322895

Mohaček-Grošev, V., Božac, R., and Puppels, G.J., 2001. Vibrational spectroscopic characterization of wild growing mushrooms and toadstools. Spectrochimica Acta Part A: Molecular and Biomolecular Spectroscopy, 57(14), 2815-2829. https://doi.org/10.1016/s1386-1425(01)00584-4

Morin-Crini, N., Loiacono, S., Placet, V., Torri, G., Bradu, C., Kostić, M., Cosentino, C., Chanet, G., Martel, B., Lichtfouse, E. and Crini, G., 2018. Hemp-based adsorbents for sequestration of metals: A review. Environmental Chemistry Letters, 17(1), 393-408. https://doi.org/10.1007/s10311-018-0812-x

Naumann, A., 2015. Fourier Transform Infrared (FTIR) Microscopy and Imaging of Fungi. Fungal Biology Advanced Microscopy in Mycology, 61-88. https://doi.org/10.1007/978-3-319-22437-4_4

Naumann, A., Navarro-González, M., Peddireddi, S., Kües, U., and Polle, A., 2005. Fourier transform infrared microscopy and imaging: Detection of fungi in wood. Fungal Genetics and Biology, 42(10), 829-835. https://doi.org/10.1016/j.fgb.2005.06.003

Njoki, M.A., Mercy, G., Nyagah, G. and Gachanja, A., 2016. Fourier transform infrared spectrophotometric analysis of functional groups found in Ricinus communis L. and Cucurbita maxima LAM. Roots, stems and leaves as heavy metal adsorbents. International Journal of Science, Environment and Technology, 5(3), 861-871. https://www.ijset.net/journal/944.pdf

Obuseng, V., Nareetsile, F. and Kwaambwa, H.M., 2012. A study of the removal of heavy metals from aqueous solutions by *Moringa oleifera* seeds and amine-based ligand 1,4-bis[N,N-bis(2-picoyl)amino]butane. Analytica Chimica Acta, 730, 87-92. https://doi.org/10.1016/j.aca.2012.01.054

Pagnanelli, F., Viggi, C., Mainelli, S. and Toro, L., 2009. Assessment of solid reactive mixtures for the development of biological permeable reactive barriers. Journal of Hazardous

Materials, 170(2-3), 998-1005.
https://doi.org/10.1016/j.jhazmat.2009.05.081

Putra, W.P., Kamari, A., Yusoff, S.N., Ishak, C.F., Mohamed, A., Hashim, N., and Isa, I.M., 2014. Biosorption of Cu(II), Pb(II) and Zn(II) Ions from Aqueous Solutions Using Selected Waste Materials: Adsorption and Characterisation Studies. Journal of Encapsulation and Adsorption Sciences,04(01), 25-35.
https://doi.org/10.4236/jeas.2014.41004

Ramrakhiani, L., Ghosh, S. and Majumdar, S., 2016. Surface Modification of Naturally Available Biomass for Enhancement of Heavy Metal Removal Efficiency, Upscaling Prospects, and Management Aspects of Spent Biosorbents: A Review. Applied Biochemistry and Biotechnology,180(1), 41-78.
https://doi.org/10.1007/s12010-016-2083-y

Reddy, D. H., Harinath, Y., Seshaiah, K., and Reddy, A., 2010. Biosorption of Pb(II) from aqueous solutions using chemically modified *Moringa oleifera* tree leaves. Chemical Engineering Journal, 162(2), 626-634.
https://doi.org/10.1016/j.cej.2010.06.010

Sağ, Y., 2001. Biosorption of heavy metals by fungal biomass and modeling of fungal biosorption: A review. Separation and Purification Methods, 30(1), 1-48.
https://doi.org/10.1081/SPM-100102984

Saravanan, R., and Ravikumar, L., 2015. The Use of New Chemically Modified Cellulose for Heavy Metal Ion Adsorption and Antimicrobial Activities. Journal of Water Resource and Protection, 07(6), 530-545.
https://doi.org/10.4236/jwarp.2015.76042

Say, R., Yılmaz, N., and Denizli, A., 2003a. Biosorption of Cadmium, Lead, Mercury, and Arsenic Ions by the Fungus Penicillium purpurogenum. Separation Science and Technology, 38(9), 2039-2053.
https://doi.org/10.1081/ss-120020133

Say, R., Yilmaz, N., and Denizli, A., 2003b. Removal of Heavy Metal Ions Using the Fungus Penicillium canescens. Adsorption Science and Technology, 21(7), 643-650.
https://doi.org/10.1260/026361703772776420

Shakya, M., Sharma, P., Meryem, S.S., Mahmood, Q., and Kumar, A, 2016. Heavy Metal Removal from Industrial Wastewater Using Fungi: Uptake Mechanism and Biochemical Aspects. Journal of Environmental Engineering, 142(9.
https://doi.org/10.1061/(asce)ee.1943-7870.0000983

Sriharsha, D.V., Lokesh, K.R. and Savitha, J., 2017. Immobilized fungi on Luffa cylindrica: An effective biosorbent for the removal of lead. Journal of the Taiwan Institute of Chemical Engineers, 80, 589-595.
https://doi.org/10.1016/j.jtice.2017.08.032

Stohs, S.J. and Hartman, M.J., 2015. Review of the safety and efficacy of *Moringa oleifera*. Phytotherapy Research, 29(6), 796-804.
https://doi.org/10.1002/ptr.5325

Svobodova, K. and Novotny, C., 2018. Bioreactors based on immobilized fungi: bioremediation under non-sterile conditions. Applied Microbiology and Biotechnology, 102(1), 39-46.
https://doi.org/10.1007/s00253-017-8575-z

Traoré, M., Kaal, J. and Cortizas, A.M., 2017. Differentiation between pine woods according to species and growing location using FTIR-ATR. Wood Science and Technology,52(2), 487-504.
https://doi.org/10.1007/s00226-017-0967-9

Velkova, Z., Kirova, G., Stoytcheva, M., Kostadinova, S., Todorova, K. and Gochev, V., 2018. Immobilized microbial biosorbents for heavy metals removal. Engineering in Life Sciences, 18, 871-881.
https://doi.org/10.1002/elsc.201800017

Wong, D., Merrifield-Macrae, M. and Stillman, M., 2017. Lead(II) binding in metallothioneins. Metal Ions in Life Sciences, 17, 241-269.
https://doi.org/10.1515/9783110434330-009

Yang, Y., Yan, Z., Wang, L., Meng, Q., Yuan, Y. and Zhu, G., 2018. Constructing synergistic groups in porous aromatic frameworks for the selective removal and recovery of lead(ii) ions. Journal of Materials Chemistry A, 6(12), 5202–5207.
https://doi.org/10.1039/c8ta00382c

Zahmatkesh, M., Spanjers, H. and van Lier, J.B., 2018. A novel approach for application of white rot fungi in wastewater treatment under non-sterile conditions: immobilization of fungi on sorghum. Environmental Technology, 39(16), 2030-2040.
https://doi.org/10.1080/09593330.2017.1347718

Zhao, G., Liu, X., Ren, S., Tan, W. and Fang, G., 2018. Quantitative comparison of surface properties of enzymatic hydrolysis lignin before and after degradation. Industrial Crops and Products, 125, 468-472.
https://doi.org/10.1016/j.indcrop.2018.09.020